The Effect of Koshu Seamount on the Formation of the Kuroshio Large Meander South of Japan

Endoh, Takahiro
Research Institute for Applied Mechanics, Kyushu University

Tsujino, Hiroyuki
Oceanographic Research Department, Meteorological Research Institute

Hibiya, Toshiyuki
Department of Earth and Planetary Science, Graduate School of Science, The University of Tokyo

https://hdl.handle.net/2324/25739

出版情報：Journal of Physical Oceanography. 41 (9), pp.1624-1629, 2011-09. American Meteorological Society
バージョン：

The Effect of Koshu Seamount on the Formation of the Kuroshio Large Meander South of Japan

TAKAHIRO ENDOH

Research Institute for Applied Mechanics, Kyushu University, Fukuoka, Japan

HIROYUKI TSUJINO

Oceanographic Research Department, Meteorological Research Institute, Ibaraki, Japan

TOSHIYUKI HIBIYA

Department of Earth and Planetary Science, Graduate School of Science, The University of Tokyo, Tokyo, Japan

(Manuscript received 12 April 2011, in final form 21 June 2011)

ABSTRACT

Using an inflow–outflow numerical model, the authors demonstrate that the existence of Koshu Seamount, located about 200 km to the south of Cape Shiono-misaki, is essential in creating the large meander (LM) of the Kuroshio. When Koshu Seamount is completely smoothed out, the meander trough propagates away without being amplified to form the LM. In contrast, nearly the same LM as in the case with full topography is formed when the foot of Koshu Seamount remains without being smoothed out and also when the foot of Koshu Seamount is filled in so that the upper part of Koshu Seamount remains. A linear stability analysis applied to the model output shows that the Kuroshio becomes baroclinically most unstable when the water depth decreases offshoreward. The authors therefore conclude that the enhancement of baroclinic instability over the northern slope of Koshu Seamount is a prerequisite to the formation of the LM.

1. Introduction

It is well known that the Kuroshio path south of Japan shows remarkable bimodal features: namely, the large meander (LM) path and the nonlarge meander (NLM) path (Fig. 1; e.g., Taft 1972; Kawabe 1995). The transition from the NLM path to the LM path is triggered by the generation of a small meander off the southeastern coast of Kyushu, which then propagates eastward up to Cape Shiono-misaki in about 4 months. After passing Cape Shiono-misaki, the small meander amplifies rapidly in about one month so that the Kuroshio loops back west of the Izu–Ogasawara Ridge, leading to the formation of the LM path. The small meander generated off the southeastern coast of Kyushu is therefore often called the ‘‘trigger meander’’ (Solomon 1978).

Corresponding author address: Takahiro Endoh, Research Institute for Applied Mechanics, Kyushu University, 6-1 Kasuga-kouen, Kasuga, Fukuoka 816-8580, Japan.
E-mail: endo@riam.kyushu-u.ac.jp

DOI: 10.1175/JPO-D-11-074.1

Using a primitive equation, inflow–outflow numerical model that takes realistic topography into account, Endoh and Hibiya (2001) successfully reproduced the stream patterns observed during the transition from the NLM path to the LM path. They demonstrated that the trigger meander amplified rapidly off Cape Shiono-misaki through the interaction with the accompanying abyssal anticyclone trapped over the local topographic feature, Koshu Seamount, which is located about 200 km to the south of Cape Shiono-misaki. This abyssal anticyclone was shown to play a crucial role in intensifying the meander trough in the upper ocean via cross-frontal advection; the intensified trough further amplified the abyssal anticyclone. This suggests that baroclinic instability over Koshu Seamount is the mechanism dominating the rapid amplification of the trigger meander off Cape Shiono-misaki. Current meter moorings deployed north of Koshu Seamount (Fukasawa and Teramoto 1986) as well as the Japan Coastal Ocean Predictability Experiment (JCOPE) reanalysis data (Endoh and Hibiya 2009) support the model results by Endoh and Hibiya (2001).

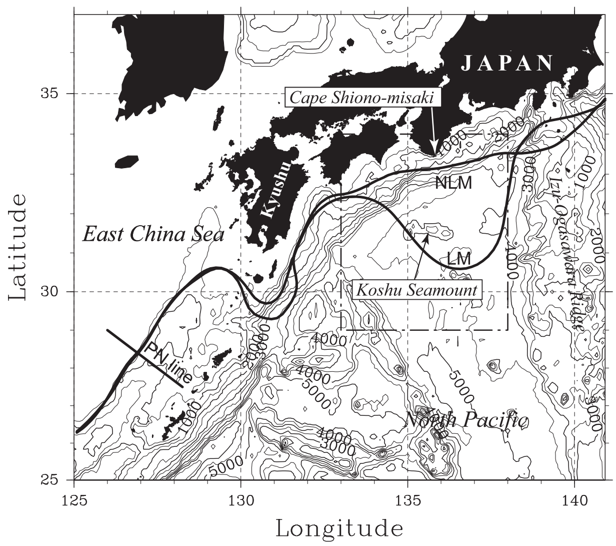

FIG. 1. Typical paths of the Kuroshio (bold lines) superposed on bathymetry of the western North Pacific and the East China Sea (contours). Contour interval is 500 m. The calculated results in the area enclosed by the dashed–dotted line are shown in Fig. 2.

Although recent model studies (Miyazawa et al. 2004; Tsujino et al. 2006) support the rapid amplification of the trigger meander through baroclinic instability as well, there is conflicting evidence as to whether the existence of Koshu Seamount is essential in creating the LM path of the Kuroshio; Endoh and Hibiya (2001) demonstrated that the meander trough was not amplified to form the LM when Koshu Seamount was removed, whereas Tsujino et al. (2006) reproduced the realistic transition from the NLM path to the LM path using an OGCM with no resolution of Koshu Seamount. However, this discrepancy is misleading because topographic configurations in Endoh and Hibiya (2001) and Tsujino et al. (2006) are different from each other, as shown in Fig. 2; the configuration of Koshu Seamount was completely smoothed out by Endoh and Hibiya (2001) (Fig. 2b), whereas Tsujino et al. (2006) used the configuration retaining the foot of Koshu Seamount falling into the Nankai Trough northward (Fig. 2c). Therefore, to obtain a definite conclusion about the role of Koshu Seamount on the formation of the LM, we have to clarify the sensitivity of the model results to changes of the configuration of Koshu Seamount.

In the present study, with the same numerical model as used by Endoh and Hibiya (2001), we carry out four sets of numerical experiments where the configuration of Koshu Seamount is altered in a systematic way, including those of the control experiments by Endoh and Hibiya (2001) and Tsujino et al. (2006). We examine the sensitivity of the model results to changes of the configuration of Koshu Seamount and obtain a definite conclusion about the role of Koshu Seamount on the formation of the LM.

2. Numerical model

A detailed description of the model configuration is given by Endoh and Hibiya (2001) so that we note here only several points that are relevant to the present study. The model domain covers the area from 20° to 40°N and from 121° to 147°E. The horizontal resolution is 18.5 km (~1/6°) in both latitudinal and longitudinal directions. In the vertical direction, we employ 30 levels that are unevenly distributed from the sea surface down to the bottom. The values of parameters are the same as used by Endoh and Hibiya (2001), except that the coefficients of the horizontal and vertical eddy diffusivities are reduced to be more widely accepted values of 100 $m^2\ s^{-1}$ and $1 \times 10^{-5}\ m^2\ s^{-1}$, respectively. The Kuroshio is driven by specifying the inflow across the southern boundary as well as the outflow across the eastern boundary; the longitude (latitude) of the current axis at the inlet (outlet) is assumed to be 122.5°E (35.5°N). The maximum current velocity at both the inlet and outlet is assumed to be 2 $m\ s^{-1}$; the resulting volume transport through the Pollution Nagasaki (PN) line in the East China Sea (see Fig. 1) is about 25 Sv (1 Sv $\equiv 10^6\ m^3\ s^{-1}$), nearly equal to the observed average value of about 24.4 Sv (Kawabe 1995).

The experimental procedure is also similar to that described by Endoh and Hibiya (2001). First, we assume a narrow jet all the way from the inlet down to the outlet, and then the model is spun up for 6840 days. Toward the end of the spinup period, transient responses die away and a quasi-stationary NLM path is attained. Then, a Gaussian-type anticyclonic mesoscale eddy with the maximum tangential current speed of 0.4 $m\ s^{-1}$ at a radius of 100 km is placed at 26.5°N and 131°E in the numerical model. As demonstrated by Endoh and Hibiya (2001), the imposed anticyclonic eddy interacts with the Kuroshio to generate the trigger meander off the southeastern coast of Kyushu (see their Fig. 5).

In the present study, we carry out four sets of numerical experiments, in total, with each changing the configuration of Koshu Seamount (Fig. 2). In experiment 1, full topography is used (Fig. 2a). Experiment 2 is the same as experiment V by Endoh and Hibiya (2001), where the configuration of Koshu Seamount is completely smoothed out (Fig. 2b). The configuration of experiment 3 is equivalent to the one in the control experiment by Tsujino et al. (2006), where the upper part of Koshu Seamount is dredged to be flat at a depth of 4350 m so that the foot of Koshu Seamount remains (Fig. 2c). In experiment 4, the foot of Koshu Seamount is filled in, whereas the upper part of Koshu Seamount remains (Fig. 2d). All of these numerical experiments are started from the quasi-equilibrium state attained in the spinup run with full topography, and the time evolution

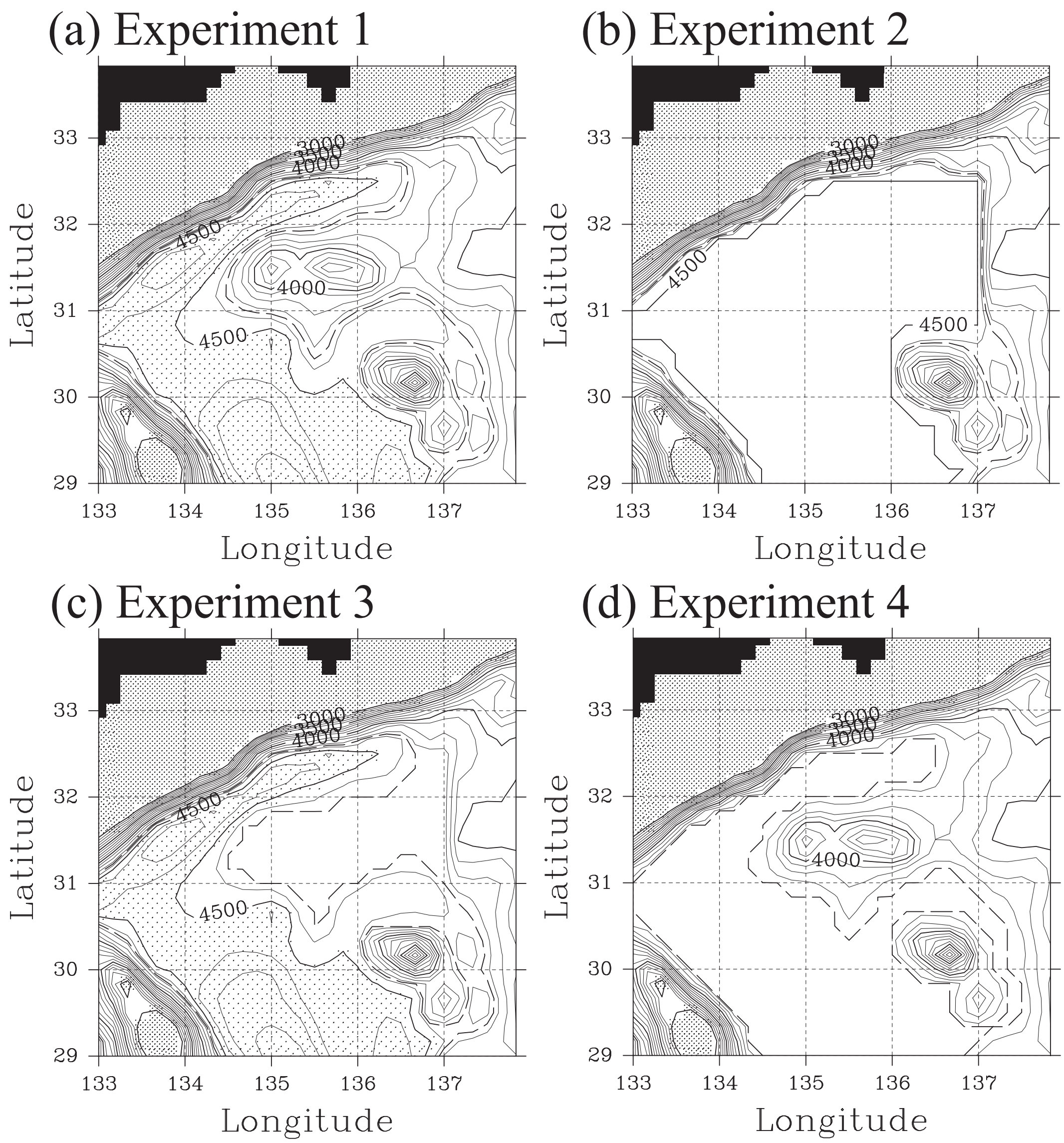

FIG. 2. Local bathymetry off Cape Shiono-misaki in (a) experiment 1, where bottom topography is derived from the 5-minute gridded elevations/bathymetry for the world (ETOPO5) dataset (National Oceanic and Atmospheric Administration 1988); (b) experiment 2, where the configuration of Koshu Seamount is completely smoothed out, as in the control experiment by Endoh and Hibiya (2001); (c) experiment 3, where the upper part of Koshu Seamount is dredged to be flat at a depth of 4350 m so that the foot of Koshu Seamount remains, as in the control experiment by Tsujino et al. (2006); and (d) experiment 4, where the foot of Koshu Seamount is filled in, whereas the upper part of Koshu Seamount remains. Contour interval is 100 m, and the dashed line shows the 4350-m isobath. Areas with water depths deeper than 4500 m (shallower than 3000 m) are light shaded (dark shaded).

of the trigger meander off Cape Shiono-misaki is compared between the numerical experiments.

3. Results

Figure 3 shows sequences of the density field at a depth of 450 m superposed on the abyssal horizontal velocity field at a depth of 3750 m off Cape Shiono-misaki for all the numerical experiments. As mentioned above, experiments 1 and 2 reproduce nearly the same results as in experiments I and V by Endoh and Hibiya (2001), respectively, with small differences resulting from the employment of the reduced coefficients of the horizontal and vertical eddy diffusivities. As demonstrated by Endoh and Hibiya (2001), the trigger meander is amplified to form the LM through the interaction with the abyssal

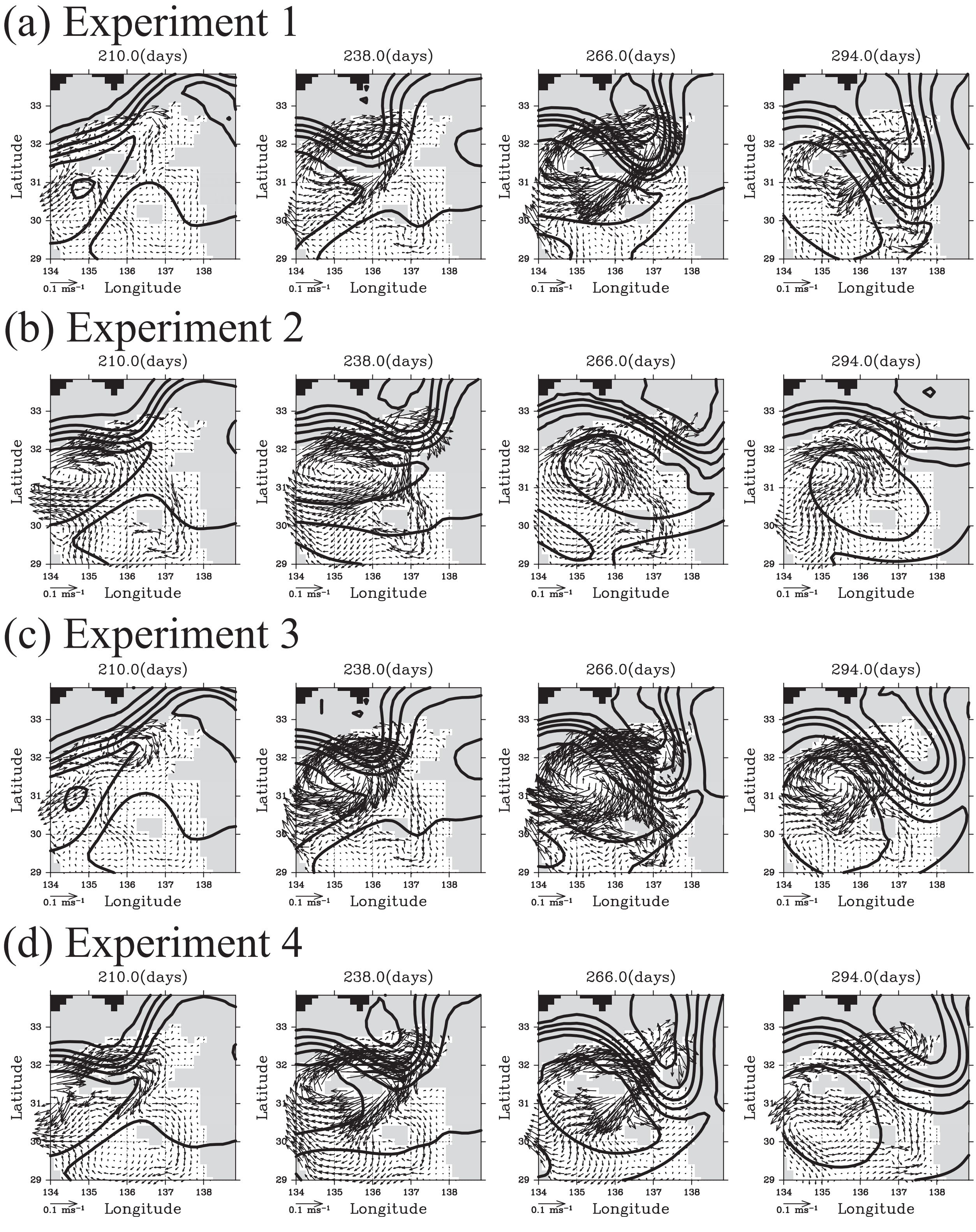

FIG. 3. Sequences of the density field at a depth of 450 m (contours) superposed on the abyssal horizontal velocity field at a depth of 3750 m (vectors) off Cape Shiono-misaki for (a) experiment 1, (b) experiment 2, (c) experiment 3, and (d) experiment 4. Contour interval for the density is 0.2 kg m^{-3}. Areas with water depths shallower than 3750 m are shaded.

anticyclone trapped over Koshu Seamount in experiment 1 (Fig. 3a), whereas the meander trough propagates away over the Izu–Ogasawara Ridge without being amplified in experiment 2, where the configuration of Koshu Seamount is completely smoothed out (Fig. 3b). In experiment 3, where the foot of Koshu Seamount remains without being smoothed out, in contrast, the abyssal anticyclone develops at nearly the same location as in experiment 1, interacting with the trigger meander to form the LM (Fig. 3c). This indicates that the discrepancy between the calculated results by Endoh and Hibiya (2001) and Tsujino et al. (2006) is due to the different way of isolating the effect of Koshu Seamount; if Tsujino et al. (2006) had used the configuration of experiment 2, they would not have reproduced the transition to the LM. Furthermore, striking resemblance of the results of experiment 4 (Fig. 3d) to those of experiments 1 and 3 implies that the slope of Koshu Seamount from the top right down to the foot plays an essential role in the formation of the LM.

To confirm this, a linear stability analysis of the trigger meander is carried out using the model output before the anticyclonic mesoscale eddy is placed. We employ the formulation based on a quasigeostrophic equation for a continuously stratified fluid (Tsujino et al. 2006) where a horizontally uniform mean flow $[U(z), V(z)]$ is assumed, bearing in mind that this is just the first-order analysis because the Kuroshio actually has a horizontal shear as well. Substituting a plane wave perturbation,

$$\phi(x, y, z, t) = F(z)\exp[i(kx + ly - \omega t)], \qquad (1)$$

into the linear quasigeostrophic equation

$$\left(\frac{\partial}{\partial t} + U\frac{\partial}{\partial x} + V\frac{\partial}{\partial y}\right)\left[\nabla^2\phi + \frac{\partial}{\partial z}\left(\frac{f_0^2}{N^2}\frac{\partial\phi}{\partial z}\right)\right] + \beta\frac{\partial\phi}{\partial x} + \frac{\partial\phi}{\partial x}\left[\frac{\partial}{\partial z}\left(\frac{f_0^2}{N^2}\frac{\partial U}{\partial z}\right)\right] - \frac{\partial\phi}{\partial y}\left[\frac{\partial}{\partial z}\left(\frac{f_0^2}{N^2}\frac{\partial V}{\partial z}\right)\right] = 0, \qquad (2)$$

where N is the buoyancy frequency and $f_0 + \beta y$ is the Coriolis parameter, we obtain an eigenvalue equation,

$$\omega\left[-K^2F + \frac{\partial}{\partial z}\left(\frac{f_0^2}{N^2}\frac{\partial F}{\partial z}\right)\right] = \left[\frac{\beta k}{K} - \frac{\partial}{\partial z}\left(\frac{f_0^2}{N^2}\frac{\partial \tilde{U}}{\partial z}\right)\right]KF + \left[-K^2F + \frac{\partial}{\partial z}\left(\frac{f_0^2}{N^2}\frac{\partial F}{\partial z}\right)\right]K\tilde{U}, \qquad (3)$$

where ω and F are the eigenvalue and the corresponding eigenvector, respectively; $K = \sqrt{k^2 + l^2}$; and $\tilde{U} = (Uk + Vl)/K$. Equation (3) is numerically solved with the boundary conditions

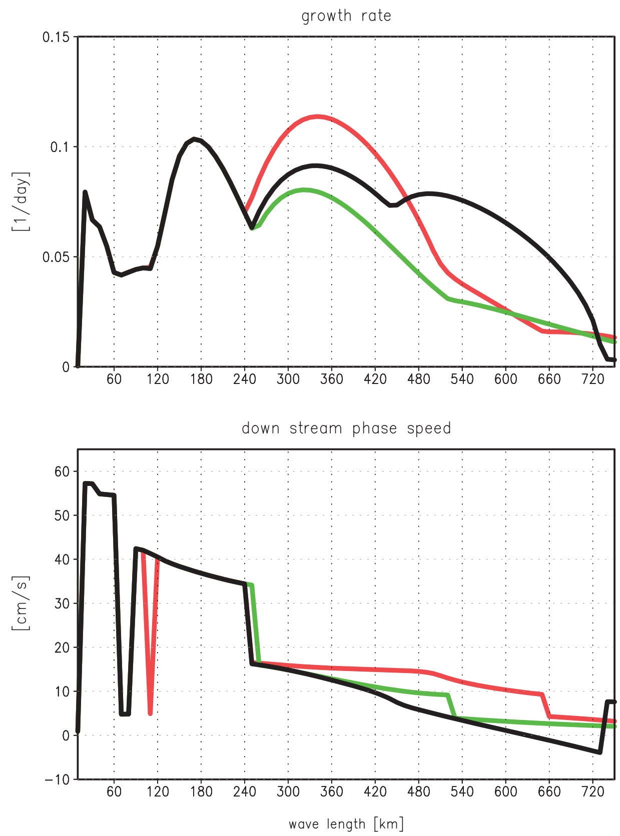

FIG. 4. (top) Growth rate and (bottom) downstream phase speed as a function of the wavelength $2\pi/K$ for the most unstable mode, which are calculated by applying a linear stability analysis to the model output. The colored lines indicate the calculated results for $\gamma = -0.002$ (red), 0 (black), and 0.002 (green). Note that the positive (negative) value of γ means that the water depth increases (decreases) offshoreward.

$$\frac{\partial F}{\partial z} = 0 \qquad \text{at} \quad z = 0\,(\mathrm{m}),$$
$$(-\omega + K\tilde{U})\frac{\partial F}{\partial z} = -\frac{N^2}{f_0}\frac{\gamma K\tilde{U}}{\sqrt{U^2 + V^2}}F \qquad \text{at} \quad z = -5000\,(\mathrm{m}), \qquad (4)$$

where γ is the gradient of a bottom slope perpendicular to the mean flow. The squared buoyancy frequency N^2 is derived by taking a horizontal average of density within the area of 32°–33.5°N and 134°–135.5°E, whereas $U(z)$ and $V(z)$ are calculated by taking the projection of the horizontal velocities averaged within the same area onto the direction of the vertically integrated velocity of them.

Figure 4 shows the calculated growth rate and downstream phase speed of the most unstable mode for $\gamma = -0.002$ (red), 0 (black), and 0.002 (green). Note that the positive (negative) value of γ means that the water depth increases (decreases) offshoreward. For the typical wavelength of the trigger meander ($2\pi/K$ = 300–420 km), we can find that the Kuroshio becomes most unstable over the negative bottom slope, although the downstream phase speed is fairly independent on the bottom slope. The sensitivity of the growth rate to the bottom slope is qualitatively consistent with the results of the present numerical experiments, indicating that the enhancement of baroclinic instability over the northern slope of Koshu Seamount is a prerequisite to the amplification of the trigger meander and hence the formation of the LM path of the Kuroshio.

4. Concluding remarks

There is an argument on whether the existence of Koshu Seamount, located about 200 km to the south of Cape Shiono-misaki, is essential in creating the LM path of the Kuroshio south of Japan (Endoh and Hibiya 2001; Tsujino et al. 2006). Using a primitive equation inflow–outflow numerical model, we have demonstrated that this discrepancy is caused by the different way of isolating the effect of Koshu Seamount. When the configuration of Koshu Seamount is completely smoothed out as in the control experiment by Endoh and Hibiya (2001), the meander trough propagates away over the Izu–Ogasawara Ridge without being amplified to form the LM. In contrast, nearly the same LM path as in the case for the full configuration of Koshu Seamount is formed when the foot of Koshu Seamount remains without being smoothed out as in the control experiment by Tsujino et al. (2006) and also when the foot of Koshu Seamount is filled in so that the upper part of Koshu Seamount remains. These results imply that the slope of Koshu Seamount plays an essential role in the formation of the LM. In fact, a linear stability analysis applied to the model output has shown that the Kuroshio becomes baroclinically most unstable when the water depth decreases offshoreward, qualitatively consistent with the results of the present numerical experiments.

The main conclusion derived from these results is that the enhancement of baroclinic instability over the northern slope of Koshu Seamount is a prerequisite to the formation of the LM path of the Kuroshio. This is consistent with the observed result that the transition from the NLM path to the LM path occurred only when the amplitude of the small meander off Cape Shiono-misaki was large enough for the meander trough to reach over the northern slope of Koshu Seamount (Ambe et al. 2009).

Although the amplitude of the small meander in the present numerical model is strongly dependent on the strength of the imposed anticyclonic mesoscale eddy (Endoh and Hibiya 2001), the reanalysis data during the transition from the NLM path to the LM path in 2004 show that the interaction between the Kuroshio and the approaching mesoscale eddies is much more complicated than previously thought (Usui et al. 2008; Miyazawa et al. 2008). More in situ observations combined with numerical studies are indispensable to clarify the generation mechanism of the trigger meander.

Acknowledgments. The authors express their gratitude to two anonymous reviewers for invaluable comments on the original manuscript. This work was supported through a Grant-in-Aid for Scientific Research provided to T. Endoh by the Ministry of Education, Culture, Sports, Science and Technology (MEXT) of Japan (19740285 and 21740345).

REFERENCES

Ambe, D., T. Endoh, T. Hibiya, and S. Imawaki, 2009: Transition to the large meander path of the Kuroshio as observed by satellite altimetry. *La Mer,* **47,** 19–27.

Endoh, T., and T. Hibiya, 2001: Numerical simulation of the transient response of the Kuroshio leading to the large meander formation south of Japan. *J. Geophys. Res.,* **106,** 26 833–26 850.

——, and ——, 2009: Interaction between the trigger meander of the Kuroshio and the abyssal anticyclone over Koshu Seamount as seen in the reanalysis data. *Geophys. Res. Lett.,* **36,** L18604, doi:10.1029/2009GL039389.

Fukasawa, M., and T. Teramoto, 1986: Characteristics of deep currents off Cape Shiono-misaki before and after formation of the large meander of the Kuroshio in 1981. *J. Oceanogr. Soc. Japan,* **42,** 53–68.

Kawabe, M., 1995: Variations of current path, velocity, and volume transport of the Kuroshio in relation with the large meander. *J. Phys. Oceanogr.,* **25,** 3103–3117.

Miyazawa, Y., X. Guo, and T. Yamagata, 2004: Roles of mesoscale eddies in the Kuroshio paths. *J. Phys. Oceanogr.,* **34,** 2203–2222.

——, T. Kagimoto, X. Guo, and H. Sakuma, 2008: The Kuroshio large meander formation in 2004 analyzed by an eddy-resolving ocean forecast system. *J. Geophys. Res.,* **113,** C10015, doi:10.1029/2007JC004226.

National Oceanic and Atmospheric Administration, 1988: ETOPO5 digital relief of the surface of the earth. NOAA/National Geophysical Data Center. [Available online at http://www.ngdc.noaa.gov/mgg/global/etopo5.HTML.]

Solomon, H., 1978: Occurrence of small ''trigger'' meanders of the Kuroshio off southern Kyushu. *J. Oceanogr. Soc. Japan,* **34,** 81–84.

Taft, B. A., 1972: Characteristics of the flow of the Kuroshio south of Japan. *Kuroshio: Its Physical Aspects,* H. Stommel and K. Yoshida, Eds., University of Tokyo Press, 165–216.

Tsujino, H., N. Usui, and H. Nakano, 2006: Dynamics of Kuroshio path variations in a high-resolution general circulation model. *J. Geophys. Res.,* **111,** C11001, doi:10.1029/2005JC003118.

Usui, N., H. Tsujino, H. Nakano, and Y. Fujii, 2008: Formation process of the Kuroshio large meander in 2004. *J. Geophys. Res.,* **113,** C08047, doi:10.1029/2007JC004675.